Multi-Sensor Data Fusion for UAV Navigation during Landing Operations

Xilin Yang*, Luis Mejias*, and Matt Garratt**

*Australian Research Center for Aerospace Automation, Queensland University of Technology, Brisbane, Australia. Email:{xilin.yang, luis.mejias}@qut.edu.au
**School of Engineering and Information Technology, University of New South Wales at the Australian Defence Force Academy, Canberra, Australia.
Email:{m.garratt}@adfa.edu.au

November 16, 2011

Abstract

This paper presents a practical framework to synthesize multi-sensor navigation information for localization of a rotary-wing unmanned aerial vehicle (RUAV) and estimation of unknown ship positions when the RUAV approaches the landing deck. The estimation performance of the visual tracking sensor can also be improved through integrated navigation. Three different sensors (inertial navigation, Global Positioning System, and visual tracking sensor) are utilized complementarily to perform the navigation tasks for the purpose of an automatic landing. An extended Kalman filter (EKF) is developed to fuse data from various navigation sensors to provide the reliable navigation information. The performance of the fusion algorithm has been evaluated using real ship motion data. Simulation results suggest that the proposed method can be used to construct a practical navigation system for a UAV-ship landing system.

1 INTRODUCTION

RUAVs have received increasing interest in the past few decades. Compared with their fixed-wing counterparts, maneuverability of RUAVs is significantly improved due to the particular structural and aerodynamic characteristics. The resultant operational flexibility, including vertical take-off and landing capability, hover at a desired height, longitudinal and lateral manoeuvre, etc., makes RUAVs an indispensable platform to perform a variety of applications such as surveillance and reconnaissance, search and rescue, urgent cargo transportation, and scientific investigations on specified ocean areas or volcanoes. There is also a growing desire to operate RUAVs in a maritime environment which introduces new challenges owing to the adverse turbulence over the flight deck, variational ship motion through waves, and the induced interactions when the RUAV approaches the superstructure of the ship. A successful automatic landing of a RUAV requires highly accurate navigation capability to plan a smooth trajectory, which results from its vulnerability to impact forces during touchdown caused by its small size and random deck motion.

The combination of various navigation sensors provides a feasible means of achieving high accuracy whilst reducing the cost. Integrated navigation system makes significant efforts to take advantage of auxiliary attributes of multiple sensors for the purpose of estimation enhancement with a better accuracy. The current integrated navigation system

carried onboard our RUAV comprises three measurement sensors: Inertial Navigation Sensor (INS), GPS, and Tracking Sensor (TS). GPS/INS are combined complementarily to estimate translational positions and velocities of the RUAV. For an automatic landing, of particular interest are ship positions and attitudes which are not directly available for the RUAV. However, they can be estimated if instantaneous relative position information between the ship and the RUAV is measured properly. Therefore, an auxiliary TS can be used onboard the RUAV [6], providing consistently relative positions. The fusion of INS, GPS, and TS makes it feasible to provide navigation information with satisfactory precision by developing effective filtering algorithms that account for noisy measurements, and estimate ship motion dynamics. Moreover, the effective estimation of ship positions facilitates extraction of the monotonous trend of the landing deck, relieving the RUAV of changing its height to track the instantaneous deck dynamics which would cause substantive consumption of power.

The GPS/INS synergy strategy is an efficient integration able to operate in a wide range of scenarios and provides low-cost high-accuracy estimation performance, and has been discussed extensively in a number of articles [11, 2, 3, 12]. Dittrich *et al.* [2] considered design and development of a practical avionics system which can provide reliable navigation information for the flight computer of an autonomous helicopter. The navigation system was constructed using the extended Kalman filtering technique by fusing measurements from GPS, IMU, sonar and radar altimeters. A family of nonlinear Kalman filters called sigma-point Kalman filter was presented for integrated navigation in [10]. It was reported that the proposed Kalman filter can capture the posterior mean and covariance more accurately, and its implementation was often substantially easier than the EKF. The example given in this paper showed an approximate 30% error reduction in attitudes and positions can be achieved compared with the EKF when the proposed method was applied to a rotorcraft platform. Zhang *et al.* [13] presented a navigation system for an autonomous vehicle by integrating measurements from IMU, GPS and digital compass. To overcome low precision of separate sensors, system estimation was implemented by using the unscented Kalman filter which had a higher calculation accuracy compared with the EKF. The unscented Kalman filter is a derivative-free variant of Kalman filter and can capture the posterior mean and covariance accurately to the third-order (Taylor series expansion) for nonlinear systems [10]. Implementation of the unscented Kalman filter requires a set of weighted sigma points to be chosen such that certain properties of these points match those of the prior distributions [9]. Also, additional weight parameters should be selected according to the type of sigma-point approach used [10]. Therefore, implementation of the unscented Kalman filter requires careful choice of weight parameters, and it is time-consuming to obtain these parameters by implementing the nonlinear unscented transformation online for a flight computer performing multiple tasks during flight operations. In our case, we are targeting a feasible filtering approach which can be implemented easily at the cost of limited flight computer memory and provide sufficient estimation accuracy. Also, due to the fact that introduction of high order (second order and higher orders) system dynamics does not generally lead to an improvement in system performance [5], we use the EKF in this paper to perform the sensor fusion task.

In the considered application, positions and velocities of the RUAV can be estimated accurately through combination of GPS and INS. For automatic landing, of particular interest are ship positions which cannot be measured by the RUAV. However, they can be estimated if the relative position information between the ship and the RUAV is obtained.

The following paper proposes a novel and feasible systematic framework for estimating unknown ship position in an automatic landing system for RUAVs. The sensor fusion approach relies on relatively low-cost sensors and yields estimation results with high accuracy. This eliminates the dependency on expensive high-accuracy sensors during this type of tasks. The combination with high-intensity color tracking sensors guarantees that the proposed sensor fusion algorithm can be applied during the night or in a gusty environment, which extends applicability of the proposed method to a large number of maritime flight

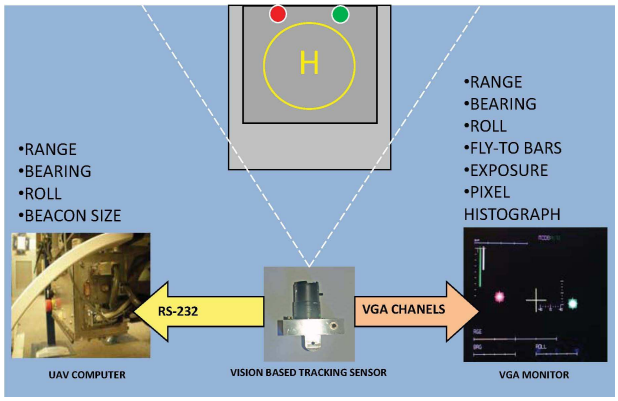

Figure 1: Vision based tracking sensor [8]

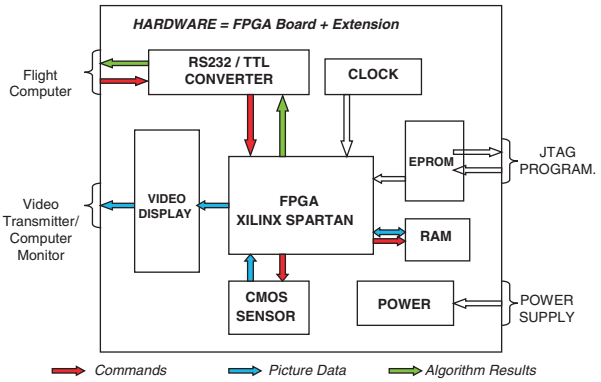

Figure 2: Structure of the tracking sensor hardware

operations.

This paper is organised as follows: In Section 2 we provide a description of the tracking sensor used in our approach. In Section 3 we present the mathematical formulation of the sensor fusion approach. Section 4 depicts the simulation results obtained, and finally some brief conclusions are presented in Section 5.

2 Tracking Sensor

The combination of IMU/GPS is able to give satisfactory estimation of helicopter positions. However, ship positions are unknown. To provide the missing information, a visual tracking sensor has been developed which can give relative motion information between a RUAV and the ship deck.

In previous work, Garratt *et al.* [4] developed a system of three visual landmarks on the ground to control a small RUAV in hover. The tracking system suffers from the problem of losing track when it is used for tracking landmarks on an oscillating ship deck. This results from the possibility that the sea spray could obscure parts of a visual pattern or parts of the pattern disappear from the field of view frequently due to the combined motion of the RUAV and the ship.

To improve the estimation accuracy, two colored *beacons* are employed with known configuration information [8], as shown in Fig. 1. The use of color enables the left and right beacons to be discriminated. The combination of a digital camera and a target detection algorithm can provide reliable relative motion information between a RUAV and a ship deck. The relative motion information can be obtained by tracking the motion of the center of the two beacons. Range, azimuth and elevation are functions of the frame coordinates of the captured images (center of the beacons) within the field of view. The relative range can be derived based on the beacon horizontal separation information and positions of the heading pointer within the frame [8].

The structure of the tracking sensor hardware is depicted in Fig. 2. The beacon tracking system is lightweight, self-contained, and consumes low power. The employment of a mega-pixel CMOS image sensor makes it possible to combine all of the necessary image processing and coordinate determination within a single *Xilinx Spartan* IIE Field Programmable Gate Array (FPGA). The FPGA interfaces to the flight control system using RS232 serial communications, and provides extra diagnostics to an external monitor. The preliminary tests have shown that robust color segmentation and accurate target coordinate generation are achieved with minimal use of FPGA resources [8]. Additionally, the data generated from

the tracking algorithm can be used to obtain an accurate estimate of the relative range up to 30 m.

3 Sensor Fusion Algorithm using the EKF

To derive the system update equations and measurement equations for the EKF, two sets of coordinate frames (body frame and navigation frame) are defined for coordinate transformation, as illustrated in Fig. 3. The body frame is fixed orthogonally to the origin O_b located at the Center of Gravity (CG) with axis set aligned with the roll, pitch and yaw axes of the RUAV. The INS and TS are installed with respect to the body frame. The second coordinate frame, also referred to as the North-East-Down (NED) coordinate frame, defines its origin O_n at the location of the navigation system where a proper navigation solution is found out. Its orthogonal axes align with the directions of north, east, and the local vertical (down) [11, 7].

The structure of the integrated navigation scheme is shown in Fig. 4. Due to the fact that the GPS-based receiver is susceptible to jamming in a dynamic environment and velocity measurements from the GPS are also noisy owing to variations in signal strength, the effects of changing multi-path and user lock instability [11], it is necessary to incorporate the INS into the navigation system to yield benefits over operating the GPS alone. Normally, measurements from different sensors require calibrations before the sensor fusion is performed. The GPS onboard uses a Novatel OEM4-G2L GPS cards which perform differential corrections. In the IMUs used in these sort of projects (e.g. Crossbow NAV-440, NovAtel SPAN), corrections for offsets and other errors are already compensated inside these commercially available systems. Hence further error compensation is not warranted for the attitude and rate states. The major source of errors is in the position and velocity estimates and we address these issues in our sensor fusion paradigm. Standard deviations of noise levels in measurements of azimuth and elevation angles from the visual tracking sensor are 0.18^o, which is accurate enough to be used for sensor fusion. The proposed sensor fusion algorithm aims to smooth out noise in RUAV position and velocity measurements. Besides, it serves to estimate deck displacement by fusing the following groups of measurements: helicopter positions (x_h, y_h, z_h) and velocities (v_{xh}, v_{yh}, v_{zh}) from GPS, relative motion information (α_r, β_r, d_r) described in spherical coordinates from TS, and helicopter accelerations (a_x, a_y, a_z) and angular rates (p, q, r) from INS. Here, helicopter velocities (u, v, w) in body frame are related to velocities (v_{xh}, v_{yh}, v_{zh}) in navigation frame by the direction cosine matrix C_b^n

$$[v_{xh}, v_{yh}, v_{zh}]^T = C_b^n \, [u, v, w]^T \tag{1}$$

with C_b^n expressed in quaternion parameters (see page 7) [11]. Here, quaternion elements are denoted by $\boldsymbol{q} = [q_0, q_1, q_2, q_3]^T$. The quaternion attitude expression is a four-element representation based on the viewpoint that a transformation from one frame to another can be interpreted as a single rotation about a vector defined with respect to the reference frame [11]. The singular problems encountered when attitudes are expressed in Euler forms can be avoided via adoption of the quaternion form.

The discrete-time system updating model of EKF takes the form of

$$X_k = f(X_{k-1}, k-1) + \varepsilon_k \tag{2}$$

where state vector X corresponds to 17 state variables

$$X = [x_h, y_h, z_h, u, v, w, x_s, y_s, z_s, v_{xs}, v_{ys}, v_{zs}, x_r, y_r, z_r, \psi_s, V_{\psi s}]^T \tag{3}$$

and system noise (mutually independent with Gaussian distributions) is $\varepsilon = [\varepsilon_1, \cdots, \varepsilon_{17}]^T$.

Here, RUAV positions (x_h, y_h, z_h), ship positions (x_s, y_s, z_s) and velocities (v_{xs}, v_{ys}, v_{zs}), and relative positions (x_r, y_r, z_r) are in navigation frame. Ship yaw and yaw rate are denoted by ψ_s and $V_{\psi s}$. The RUAV can receive ship heading (yaw) information from radio signals sent by the ship. Equation (3) can

be expressed in an explicit form

$$(x_h)_k = (x_h)_{k-1} + T_s[(c_{11})_{k-1}u_{k-1} + (c_{12})_{k-1}v_{k-1} + (c_{13})_{k-1}w_{k-1}] + (\varepsilon_1)_k \quad (4)$$

$$(y_h)_k = (y_h)_{k-1} + T_s[(c_{21})_{k-1}u_{k-1} + (c_{22})_{k-1}v_{k-1} + (c_{23})_{k-1}w_{k-1}] + (\varepsilon_2)_k \quad (5)$$

$$(z_h)_k = (z_h)_{k-1} + T_s[(c_{31})_{k-1}u_{k-1} + (c_{32})_{k-1}v_{k-1} + (c_{33})_{k-1}w_{k-1}] + (\varepsilon_3)_k \quad (6)$$

$$u_k = u_{k-1} + T_s[r_{k-1}v_{k-1} - q_{k-1}w_{k-1} + (a_x)_{k-1}] + (\varepsilon_4)_k \quad (7)$$

$$v_k = v_{k-1} + T_s[-r_{k-1}u_{k-1} + p_{k-1}w_{k-1} + (a_y)_{k-1}] + (\varepsilon_5)_k \quad (8)$$

$$w_k = w_{k-1} + T_s[q_{k-1}u_{k-1} - p_{k-1}v_{k-1} + (a_z)_{k-1}] + (\varepsilon_6)_k \quad (9)$$

$$(x_s)_k = (x_s)_{k-1} + T_s(v_{xs})_{k-1} + (\varepsilon_7)_k \quad (10)$$

$$(y_s)_k = (y_s)_{k-1} + T_s(v_{ys})_{k-1} + (\varepsilon_8)_k \quad (11)$$

$$(z_s)_k = (z_s)_{k-1} + T_s(v_{zs})_{k-1} + (\varepsilon_9)_k \quad (12)$$

$$(v_{xs})_k = (v_{xs})_{k-1} + (\varepsilon_{10})_k \quad (13)$$

$$(v_{ys})_k = (v_{ys})_{k-1} + (\varepsilon_{11})_k \quad (14)$$

$$(v_{zs})_k = (v_{zs})_{k-1} + (\varepsilon_{12})_k \quad (15)$$

$$(x_r)_k = (x_r)_{k-1} + (\varepsilon_{13})_k \quad (16)$$

$$(y_r)_k = (y_r)_{k-1} + (\varepsilon_{14})_k \quad (17)$$

$$(z_r)_k = (z_r)_{k-1} + (\varepsilon_{15})_k \quad (18)$$

$$(\psi_s)_k = (\psi_s)_{k-1} + T_s(V_{\psi s})_{k-1} + (\varepsilon_{16})_k \quad (19)$$

$$(V_{\psi s})_k = (V_{\psi s})_{k-1} + (\varepsilon_{17})_k \quad (20)$$

Eq. (4)-(20) propagate states variables from time instant $k-1$ to k, and sampling time is denoted by T_s. System noise $\varepsilon_{(\cdot)}$ and covariance matrix of system noise $Q_{(\cdot)}$ satisfies

$$E\{\varepsilon^i_{(\cdot)}[\varepsilon^j_{(\cdot)}]^T\} = \delta(i-j)Q_{(\cdot)} \quad (21)$$

where δ is Kronec function taking the form of

$$\delta(i-j) = \begin{cases} 1 & \text{if } i = j \\ 0 & \text{if } i \neq j \end{cases}$$

Eq. (4)-(6) describe relationship of velocities between body frame and navigation frame. Local velocity propagations are revealed in Eq. (7)-(9) with knowledge of accelerations (a_x, a_y, a_z). In the considered application, it is not possible to build up an accurate ship motion model. However, it is reasonable to assume ship speed remains constant in forward and sideways directions during landing phase, as is shown in Eq. (10)-(15). Of particular significance is local displacement motion greatly affecting magnitude of the impact force during touchdown moment. Deck displacement speed is tentatively set to be constant, and it will be demonstrated later that the EKF is able to estimate the displacement motion effectively as relative motion (α_r, β_r, d_r) provided by TS can correct the estimation performance.

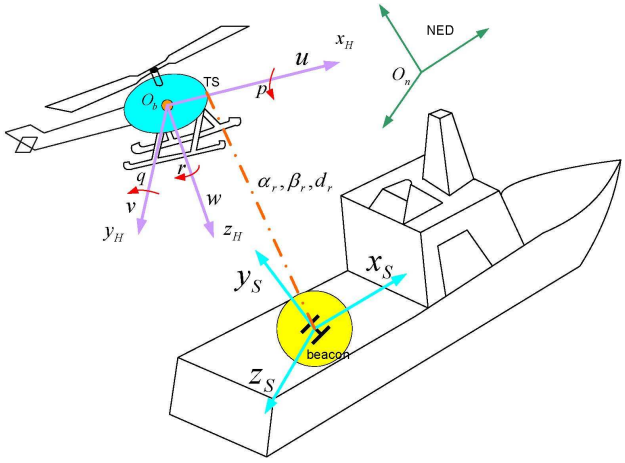

Figure 3: Frame relationship between body frame and navigation frame

Nonlinearities in system model Eq. (2) stem from the quaternion components c_{ij} in direction cosine matrix C^n_b, which should be linearized when deriving the state transition matrix $\Phi_{k|k-1}$. The differential equations for quaternion attitude in continuous-time are [5]

$$\begin{bmatrix} \dot{q}_0 \\ \dot{q}_1 \\ \dot{q}_2 \\ \dot{q}_3 \end{bmatrix} = -\frac{1}{2}\begin{bmatrix} 0 & p & q & r \\ -p & 0 & -r & q \\ -q & r & 0 & -p \\ -r & -q & p & 0 \end{bmatrix}\begin{bmatrix} q_0 \\ q_1 \\ q_2 \\ q_3 \end{bmatrix} = -\frac{1}{2}\Omega \boldsymbol{q} \quad (22)$$

For a sufficiently small sampling time interval T_s, Eq. (22) can be linearized using the first-order approxi-

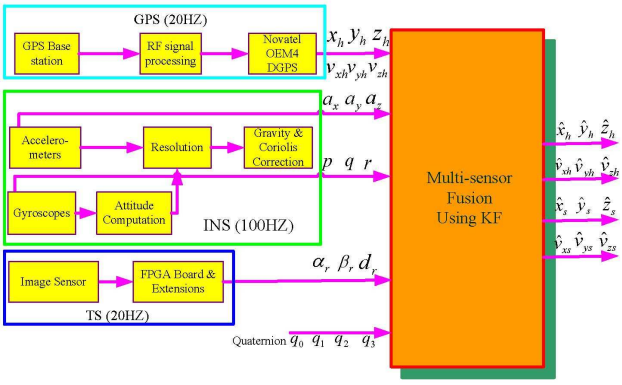

Figure 4: Architecture of EKF for multi-sensor fusion

mation

$$\Delta \boldsymbol{q} \approx -\frac{1}{2}\Omega \boldsymbol{q} T_s \tag{23}$$

Since it is expected to determine the change of vectors relative to the body frame, then quaternion vector is set to be $\boldsymbol{q} = [1\ 0\ 0\ 0]^T$. Following Eq. (22), the change in attitude over the time interval T_s is given by

$$\begin{bmatrix} \Delta q_0 \\ \Delta q_1 \\ \Delta q_2 \\ \Delta q_3 \end{bmatrix} \approx \begin{bmatrix} 0 \\ pT_s/2 \\ qT_s/2 \\ rT_s/2 \end{bmatrix} \tag{24}$$

and the change in attitude over the time interval relative to body frame is

$$\begin{bmatrix} q_0 \\ q_1 \\ q_2 \\ q_3 \end{bmatrix} = \begin{bmatrix} 1 \\ pT_s/2 \\ qT_s/2 \\ rT_s/2 \end{bmatrix} \tag{25}$$

Defining

$$\tilde{P} \triangleq \frac{pT_s}{2}, \quad \tilde{Q} \triangleq \frac{qT_s}{2}, \quad \tilde{R} \triangleq \frac{rT_s}{2} \tag{26}$$

the rotation matrix C_b^n can be recast as (27) (see next page).

Substituting Eq. (27) into Eq. (4)-(6) leads to Eq. (28)-(30)(see next page). Therefore, the state transition matrix $\Phi_{k|k-1}$ can be derived by differentiating Eq. (28)-(30) and Eq. (7)-(20) with respect to each state. Here, the angular rates at time instant k are described by p_k, q_k, r_k. In our case, the body rate information obtained from the INS has been filtered and can be used for sensor fusion. Angular rates (p_k, q_k, r_k) do not remain constant and keep updating when measurements from the INS change.

The measurement model can be described by

$$Z_k = h(X_k, k) + \epsilon_k \tag{31}$$

where 10 measurements are $Z = [x_h, y_h, z_h, v_{xh}, v_{yh}, v_{zh}, \alpha_r, \beta_r, d_r, \psi_s]^T$ and measurement noise ϵ is

$$\epsilon = [\epsilon_1, \ldots, \epsilon_{10}]^T \tag{32}$$

The detailed measurement equations are

$$(x_h)_k = (x_h)_k + (\epsilon_1)_k \tag{33}$$
$$(y_h)_k = (y_h)_k + (\epsilon_2)_k \tag{34}$$
$$(z_h)_k = (z_h)_k + (\epsilon_3)_k \tag{35}$$
$$u_k = u_k + (\epsilon_4)_k \tag{36}$$
$$v_k = v_k + (\epsilon_5)_k \tag{37}$$
$$w_k = w_k + (\epsilon_6)_k \tag{38}$$
$$(\alpha_r)_k = \arctan\{\frac{(y_r)_k}{(x_r)_k}\} + (\epsilon_7)_k \tag{39}$$
$$(\beta_r)_k = \arccos\{\frac{(z_r)_k}{\sqrt{[(x_r)_k]^2 + [(y_r)_k]^2 + [(z_r)_k]^2}}\} + (\epsilon_8)_k \tag{40}$$
$$(d_r)_k = \sqrt{[(x_r)_k]^2 + [(y_r)_k]^2 + [(z_r)_k]^2} + (\epsilon_9)_k \tag{41}$$
$$(\psi_s)_k = (\psi_s)_k + (\epsilon_{10})_k \tag{42}$$

Measurement noise $\epsilon_{(\cdot)}$ is mutually independent with Gaussian distributions, and covariance matrix of measurement noise $R_{(\cdot)}$ satisfies

$$E\{\epsilon^i_{(\cdot)}[\epsilon^j_{(\cdot)}]^T\} = \delta(i-j)R_{(\cdot)}, \tag{43}$$

Given the system model and measurement model, an EKF can be developed to fulfill the sensor fusion task by taking the following procedure [1, 7]:

Computing the prior state estimate:

$$\hat{X}_{k|k-1} = f(\hat{X}_{k-1|k-1}, k-1) \tag{44}$$

$$C_b^n = \begin{bmatrix} c_{11} & c_{12} & c_{13} \\ c_{21} & c_{22} & c_{23} \\ c_{31} & c_{32} & c_{33} \end{bmatrix} = \begin{bmatrix} q_0^2+q_1^2-q_2^2-q_3^2 & 2(q_1q_2-q_0q_3) & 2(q_1q_3+q_0q_2) \\ 2(q_1q_2+q_0q_3) & q_0^2-q_1^2+q_2^2-q_3^2 & 2(q_2q_3-q_0q_1) \\ 2(q_1q_3-q_0q_2) & 2(q_2q_3+q_0q_1) & q_0^2-q_1^2-q_2^2+q_3^2 \end{bmatrix}$$

$$C_b^n = \begin{bmatrix} 1+\tilde{P}^2-\tilde{Q}^2-\tilde{R}^2 & 2(\tilde{P}\tilde{Q}-\tilde{R}) & 2(\tilde{P}\tilde{R}+\tilde{Q}) \\ 2(\tilde{P}\tilde{Q}+\tilde{R}) & 1-\tilde{P}^2+\tilde{Q}^2-\tilde{R}^2 & 2(\tilde{Q}\tilde{R}-\tilde{P}) \\ 2(\tilde{P}\tilde{R}-\tilde{Q}) & 2(\tilde{Q}\tilde{R}+\tilde{P}) & 1-\tilde{P}^2-\tilde{Q}^2+\tilde{R}^2 \end{bmatrix} \quad (27)$$

$$(x_h)_k = (x_h)_{k-1} + T_s[(1+\frac{(p_{k-1}^2-q_{k-1}^2-r_{k-1}^2)T_s^2}{4})u_{k-1} + 2(\frac{p_{k-1}q_{k-1}T_s^2}{4} - \frac{r_{k-1}T_s}{2})v_{k-1} + 2(\frac{q_{k-1}r_{k-1}T_s^2}{4} + \frac{q_{k-1}T_s}{2})w_{k-1} + (\varepsilon_1)_k] \quad (28)$$

$$(y_h)_k = (y_h)_{k-1} + T_s[2(\frac{p_{k-1}q_{k-1}T_s^2}{4} + \frac{r_{k-1}T_s}{2})u_{k-1} + (1+\frac{(q_{k-1}^2-p_{k-1}^2-r_{k-1}^2)T_s^2}{4})v_{k-1} + 2(\frac{q_{k-1}r_{k-1}T_s^2}{4} - \frac{p_{k-1}T_s}{2})w_{k-1}] + (\varepsilon_2)_k] \quad (29)$$

$$(z_h)_k = (z_h)_{k-1} + T_s[2(\frac{p_{k-1}r_{k-1}T_s^2}{4} - \frac{q_{k-1}T_s}{2})u_{k-1} + 2(\frac{q_{k-1}r_{k-1}T_s^2}{4} + \frac{p_{k-1}T_s}{2})v_{k-1} + (1+\frac{(r_{k-1}^2-p_{k-1}^2-q_{k-1}^2)T_s^2}{4})w_{k-1}] + (\varepsilon_3)_k \quad (30)$$

Computing the predicted measurement:

$$\hat{Z}_k = h(\hat{X}_{k|k-1}, k) \quad (45)$$

Linearize system updating equations:

$$\Phi_{k|k-1} \approx \frac{\partial f(X,k-1)}{\partial X}|_{X=\hat{X}_{k-1|k-1}} \quad (46)$$

Conditioning the predicted estimate on the measurement and linearize measurement equation:

$$\hat{X}_{k|k} = \hat{X}_{k|k-1} + K_k(Z_k - \hat{Z}_k) \quad (47)$$

$$H_{k|k-1} \approx \frac{\partial h(X,k)}{\partial X}|_{X=\hat{X}_{k|k-1}} \quad (48)$$

Computing the prior covariance matrix:

$$P_{k|k-1} = \Phi_{k|k-1}P_{k-1|k-1}\Phi_{k|k-1}^T + Q_{k-1} \quad (49)$$

Computing the Kalman gain:

$$K_k = P_{k|k-1}H_{k|k-1}^T[H_{k|k-1}P_{k|k-1}H_{k|k-1}^T + R_k]^{-1} \quad (50)$$

Computing the posteriori covariance matrix:

$$P_{k|k} = \{I - K_kH_{k|k-1}\}P_{k|k-1} \quad (51)$$

The flow chart for EKF implementation is shown in Fig. 5. The EKF algorithm is implemented as a C-file S-function block in MATLAB®Simulink and can be easily integrated into the ship/helicopter landing system.

4 Simulation Results

In this section, the EKF algorithm is tested using real-time deck displacement data for a Vario heli-

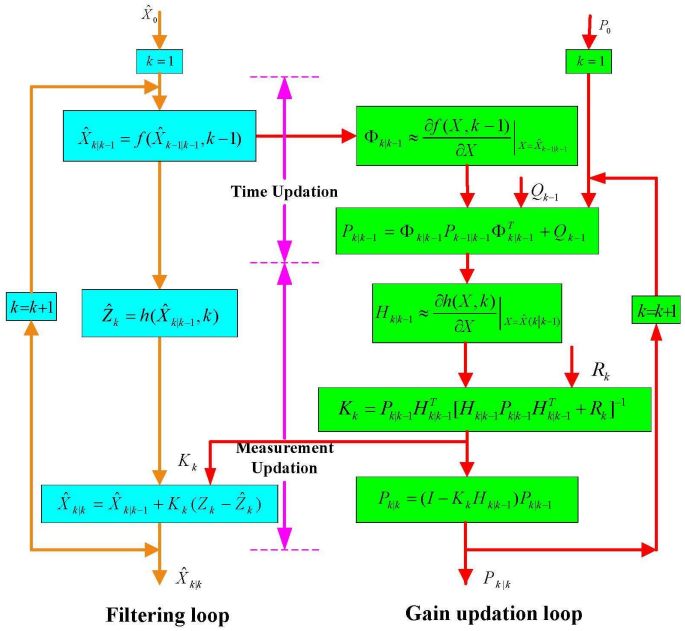

Figure 5: Flow chart for implementation of the EKF

copter model. In the simulation, the RUAV is supposed to follow the middle line of the ship, approach the deck in the constant speed of $3m/s$, and hover at a height of 10 m. For the NovAtel GPS receiver on our helicopter, the distance accuracy is 2 cm in the longitudinal-lateral plane and 4 cm in the elevation. Thus, white noise with standard deviations of $2cm$, $2cm$ and $4cm$ were added to real positions of the RUAV to test the performance of the EKF. Also, azimuth angle α_r and elevation angle β_r were contaminated by white noise with standard deviations of 0.18^o. This agrees with the noise levels in our visual tracking sensor.

Performance of the EKF when applied to estimate positions of the RUAV is shown in Fig. 6. For the sake of observation convenience, estimation results for the first 10 seconds are plotted. It is noticed that noise effects in positions are attenuated efficiently. Also, the unknown ship positions are estimated accurately, as shown in Fig. 7. Estimations of relative positions between the ship and the RUAV are given in Fig. 8. It takes around 80 seconds for the EKF to capture the system dynamics accurately. In particular, deck displacement is estimated smoothly, which greatly contributes to extracting instantaneous mean deck position for landing operations. The standard deviations of the estimated states are shown in Table 1. It is seen that the EKF can smooth out the noisy measurements and estimate ship positions effectively.

5 Conclusion

In this paper, a practical sensor fusion algorithm is proposed based on measurements from GPS, INS and tracking sensor. It employees low-cost sensors to estimate unknown ship positions with high accuracy in a dynamic environment when the RUAV approaches the landing deck. Performance of the proposed method has been evaluated using real ship motion data and simulation results demonstrate feasibility of the proposed method into real-time appli-

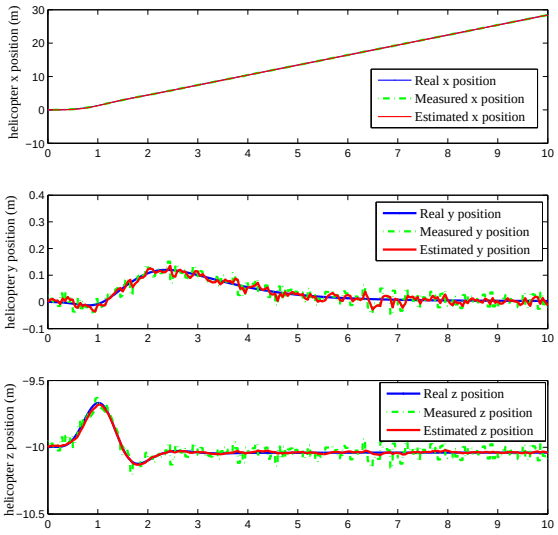

Figure 6: Estimation of RUAV positions using the EKF

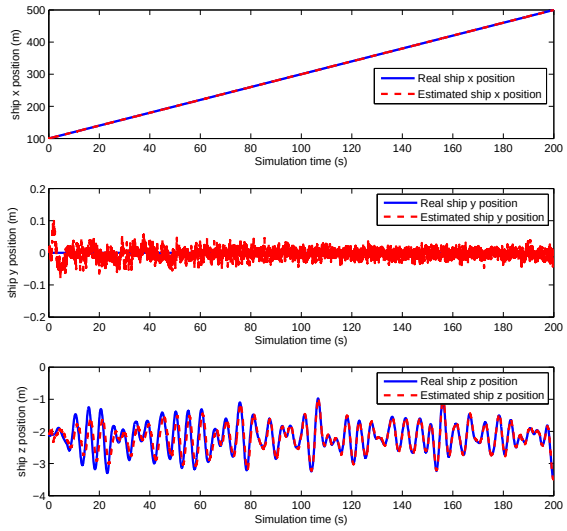

Figure 7: Estimation of ship positions using the EKF

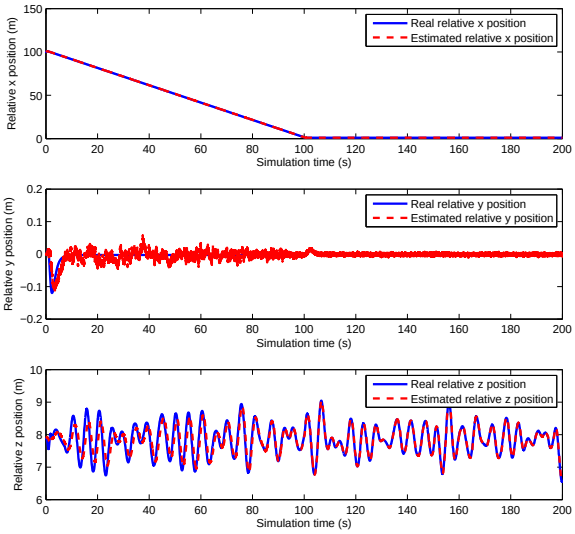

Figure 8: Estimation of relative positions

cations. The effective estimation of ship positions will facilitate extraction of the monotonous trend of the landing deck, relieving the RUAV of changing its height to track the instantaneous deck dynamics which would cause substantive consumption of power during the descent period.

References

[1] B. D. O. Anderson and J. B. Moore, *Optimal filtering*, Englewood Cliffs, N.J : Prentice-Hall, 1979.

[2] J. S. Dittrich and E. N. Johnson, *Multi-sensor navigation system for an autonomous helicopter*, Proceedings of the 21st Digital Avionics Systems Conference, vol. 2, Oct. 2002, pp. 8C1–1—8C1–9.

[3] F. A. Faruqi and K. J. Turner, *Extended kalman filter synthesis for intergrated global positioning/inertial navigation systems*, Applied Math-

Table 1: Standard deviations of the estimated states

States	Unit	Std. Dev.
x_h	m	0.15
y_h	m	0.01
z_h	m	0.02
x_s	m	0.15
y_s	m	0.01
z_s	m	0.20
x_r	m	0.04
y_r	m	0.01
z_r	m	0.19

ematics and Computation **115** (2000), no. 2-3, 213–227.

[4] M. Garratt and J. S. Chahl, *Visual control of a rotary wing UAV*, UAV Asia-Pacific Conference, Feb. 2003.

[5] M. A. Garratt, *Biologically inspired vision and control for an autonomous flying vehicle*, Ph.D. thesis, Australian National University, Australia, Oct. 2007.

[6] M. A. Garratt, H. R. Pota, A. Lambert, and S. E. Maslin, *Systems for automated launch and recovery of an unmanned aerial vehicle from ships at sea*, Proceedings of the 22nd International UAV Systems Conference (2007), 1401–1415.

[7] P. D. Groves, *Principles of GNSS, inertial, and multisensor integrated navigation systems*, Artech House, 2008.

[8] A. S. Hogg, *Development of a robust real-time colour tracking algorithm for helicopter UAV platforms*, Bachelor Thesis, Oct. 2010.

[9] S. J. Julier, *The scaled unscented transformation*, Proceedings of the American Control Conference, no. 6, 2002, pp. 4555–4559.

[10] R. V. D. Merwe and E. A. Wan, *Sigma-point kalman filters for integrated navigation*, Proceedings of the 60th Annual Meeting of the Institute of Navigation (Dayton, OH, USA), 2004, pp. 641–654.

[11] D. H. Titterton and J. L. Weston, *Strapdown inertial navigation technology*, 2 ed., vol. 207, American Institute of Aeronautics and Astronautics, 2004.

[12] J. Wendel, O. Meister, C. Schlaile, and G. F. Trommer, *An integrated GPS/MEMS-IMU navigation system for an autonomous helicopter*, Aerospace Science and Technology **10** (2006), no. 6, 527–533.

[13] P. Zhang, J. Gu, E. E. Milios, and P. Huynh, *Navigation with IMU/GPS/digital compass with unscented kalman filter*, Proceedings of the IEEE International Conference on Mechatronics & Automation (Niagara Falls, Canada), July 2005.